



---


# SELECTIVE PRUNING AND NEURONAL DEATH GENERATE HEAVY-TAIL NETWORK CONNECTIVITY

---

A PREPRINT

 **Rodrigo Kazu Siqueira\***  
Wellcome Sanger Institute  
Cambridge, England, UK  
rs47@sanger.ac.uk

 **Kleber Neves**  
Institute of Medical Biochemistry  
Federal University of Rio de Janeiro, Brazil  
kleber.neves@bioqmed.ufrj.br

 **Bruno Mota**  
Physics Institute  
Federal University of Rio de Janeiro, Brazil  
bruno@if.ufrj.br

August 6, 2024

## ABSTRACT

From the proliferative mechanisms generating neurons from progenitor cells to neuron migration and synaptic connection formation, several vicissitudes culminate in the mature brain. Both component loss and gain remain ubiquitous during brain development. For example, rodent brains lose over half of their initial neurons and synapses during healthy development. The role of deleterious steps in network ontogeny remains unclear, yet it is unlikely these costly processes are random. Like neurogenesis and synaptogenesis, synaptic pruning and neuron death likely evolved to support complex, efficient computations. In order to incorporate both component loss and gain in describing neuronal networks, we propose an algorithm where a directed network evolves through the selective deletion of less-connected nodes (neurons) and edges (synapses). Resulting in networks that display scale-invariant degree distributions, provided the network is predominantly feed-forward. Scale-invariance offers several advantages in biological networks: scalability, resistance to random deletions, and strong connectivity with parsimonious wiring. Whilst our algorithm is not intended to be a realistic model of neuronal network formation, our results suggest selective deletion is an adaptive mechanism contributing to more stable and efficient networks. This process aligns with observed decreasing pruning rates in animal studies, resulting in higher synapse preservation. Our overall findings have broader implications for network science. Scale-invariance in degree distributions was demonstrated in growing preferential attachment networks and observed empirically. Our preferential detachment algorithm offers an alternative mechanism for generating such networks, suggesting that both mechanisms may be part of a broader class of algorithms resulting in scale-free networks.

**Keywords** Scale-free · Heavy-tail connectivity · Synaptic pruning · Brain development · Neuronal death · Feed-forward networks · Preferential detachment · Power law

---

\*Kazu RS is also affiliated to the INSIGNEO Institute, University of Sheffield; Neuralpathways website & metaBIO website

## 1 Introduction

The normal process of ontogeny of the human brain is not entirely constructive. To a large extent, brain development is destructive, removing parts - neurons and synapses - generated in excess beforehand [Abitz *et al.*, 2007, Petanjek *et al.*, 2011]. It has been known for a long time that there is widespread neuronal death and synaptic pruning in the development of the nervous system [Hamburger *et al.*, 1990, Changeux and Danchin, 1976]. For instance, studies in rodents have shown that the number of neurons at birth is almost double that of the adult, with half of the initial number of neurons being eliminated by programmed cell death in the first weeks of life [Bandeira *et al.*, 2009]. While this might seem like an incredibly wasteful way of building brain circuitry, this process is thought to be a natural part of brain development and not a pathology [Clarke, 1985]. Inhibition of this regulated cell death causes differences in the number of neurons, size and shape of brains in mammals [Haydar *et al.*, 1999].

A similar phenomenon happens with synapses, albeit in a different time scale. The pruning of the initial exuberance of synapses starts early and goes on until adulthood, being necessary for normal development [Huttenlocher *et al.*, 1979, Stiles and Jernigan, 2010]. The timing and intensity of pruning, however, vary across different brain regions - e.g., sensory systems prune early as opposed to the frontal cortex that is late maturing, in this sense [Elston *et al.*, 2009]. Interestingly, this is the period thought to be when the brain is at peak plasticity [Craik and Bialystok, 2006].

Which neurons and synapses survive and which ones are eliminated?

It is well-known that the elimination of neurons and synapses is activity-dependent [Clarke, 1985, Snider *et al.*, 1992] and that synaptic pruning depends on microglial activity [Paolicelli *et al.*, 2011]. These resident immune cells are thought to make direct and ephemeral connections with synapses in a way that is quantitatively proportional to basal neuronal activity [Wake *et al.*, 2009]. Furthermore, Schafer *et al.* showed in 2012 that microglia engulf considerably more synapses of the less active cells (Tetrodotoxin-treated) as compared to untreated ones and that this tends to happen at the presynaptic terminals and relies on the microglia-specific phagocytic signalling pathway, complement receptor 3(CR3)/C3 [Schafer *et al.*, 2012].

Alterations in number/density of synapses have been shown to be associated with conditions such as autism [Thomas *et al.*, 2016, Teter *et al.*, 2024], glaucoma [Rosen and Stevens, 2010, Howell *et al.*, 2011], Huntington's disease [Wilton *et al.*, 2023], schizophrenia [Yilmaz *et al.*, 2021] and are distinguishing features of Alzheimer's disease (AD) [Hong *et al.*, 2016a, Lui *et al.*, 2016], amongst others [Hong *et al.*, 2016b, Scott-Hewitt *et al.*, 2023]. Notably, it is thought that the same mechanisms that prune excess synapses during development are inappropriately activated in AD [Hong *et al.*, 2016a].

The strengthening or weakening of synapses is thought to be regulated through Hebbian mechanisms, as in "neurons that fire together, wire together" [Hebb *et al.*, 1949]. These are the basis, for example, for the plasticity in neuronal circuits of the hippocampus [Bastrikova *et al.*, 2008] and for the experience-dependent refinement of visual circuits in the retina [Zhou *et al.*, 2004, Butts *et al.*, 2007, Zhang *et al.*, 2012]. Similarly, in the initial stages of development, neurons that are being regularly activated by peripheral innervation are the ones likely to survive. This mechanism for survival is thought to involve retrograde transport of growth factors, such as NGF and BDNF and other factors released by glial cells [Ghosh *et al.*, 1994]. Since the axonal path of every neuron cannot be specified in advance due to the sheer number of neuronal cells in the human brain [Herculano-Houzel, 2009], this is thought to be a solution to the problem of exactly finding an innervation target: project neurons in excess and remove the ones that fail to reach a target. It seems plausible that this "wasteful exuberance" is a property that was selected for, a consequence of a biophysical principle to minimize the total amount of axonal wiring [Raj and Chen, 2011].

Even though a lot is known about the function and even possible molecular and cellular mechanisms for neuronal death and synaptic pruning, the effect of these events, their timing and their order on the structure and functioning of the resulting neuronal network has not been explored.

### 1.1 Scale-invariance in neuronal networks

Our current understanding of anatomical connectivity can be traced to the late 19th century, with the postulation of the neuron doctrine. It has been since assumed that the brain is composed primarily of individual neuronal cells that are interconnected via synapses. Under this premise, the brain is a system consisting of clearly defined interconnected elements, and its functioning is determined by its observable connectivity. Mathematically, there is natural representation of such structure as a directed network of interacting nodes, to which one can apply quantitative tools and the theoretical framework borrowed from network science. This has been a fruitful approach to investigate brain activity and, far less often, its ontology. This relatively new field is called network neuroscience [Bassett and Sporns, 2017].

Functional brain connectivity studies have revealed nonrandom topological features. For example, numerous studies have identified a highly clustered cortical network characterized by short average path lengths between nodes and a small-world topology [Bullmore and Sporns, 2009, Bassett and Bullmore, 2017] (for a comprehensive review, see [Van den Heuvel *et al.*, 2016]). Additionally, significant evidence suggests that the brain network is divided into distinct communities [Puxeddu *et al.*, 2020], interconnected by metabolically expensive hub nodes [Crossley *et al.*, 2014], forming what is known as a ‘rich club’ [Van Den Heuvel and Sporns, 2011].

However, when modelling the nervous system as a network, nodes and edges can be defined at different levels, from lower (cellular or even molecular) to higher ones (large populations of cells or well-defined anatomical regions). This raises concerns that range from the experimental technique utilised for data collection to the problem of node definition [Stanley *et al.*, 2013]. Modelling the network at the cellular level adds another difficulty since experimentally mapping the details of neuronal connectivity is a significant technical challenge [Helmstaedter, 2013]. Only recently has large-scale neuronal connectivity been investigated at cellular resolution in whole organisms. These findings showed heavy-tail connectivity in the partial connectome of the *Drosophila* central brain and its optic medulla [Scheffer *et al.*, 2020, Takemura *et al.*, 2013].

Specifically, scale-free connectivity is also found in the connectome of the roundworm *Caenorhabditis elegans* [White *et al.*, 1986, Towilson *et al.*, 2013] and the sensory-motor pathways of the annelid *Platynereis* [Randel *et al.*, 2014, Lynn *et al.*, 2024]. In vertebrates, evidence for heavy-tail connectivity was found in the mouse retina both for number and size distribution of physical contacts in between neurons [Stringer *et al.*, 2019, Lynn *et al.*, 2024]. These studies collectively highlight the prevalence of heavy-tail connectivity in neuronal networks across different species.

The presence of scale-free connectivity suggests that a small fraction of neurons are significantly more connected than the majority, indicating a non-random organization that likely plays a crucial role in network dynamics and information processing within these neural circuits [Barabási, 2009]. We can infer that neuronal networks will be robust to random loss of neurons, since neuronal loss with ageing occurs, at a slow but steady rate, throughout all adulthood [Mortera and Herculano-Houzel, 2012]. This suggests that at a low level, it is plausible that neuronal networks are scale-invariant, with a degree distribution (the distribution of the number of connections of each neuronal cell) following a power law.

Known mechanisms to generate scale-free networks involve preferential attachment [Barabási and Albert, 1999, Bianconi and Barabási, 2001, Bell *et al.*, 2017]. Nodes in the network connect preferentially to the nodes with the highest intrinsic fitness or connectivity. However, this class of algorithms is not plausible biologically: neurons would require global information on the fitness and/or connectivity of other neurons [Nicosia *et al.*, 2013].

To explore the effects that the aforementioned ontogenetic events might have on the low-level organization of neuronal networks, here we take as our object of study an idealized cortical circuit [Douglas *et al.*, 1989] and perform our investigation through computational modelling. We devised a modular, evolving, and directed network of 50,000 neurons and 5,000,000 synapses. This was thought to roughly double both the number of cells in cortical columns that were reported to have 19,000 cells in mice [Meyer *et al.*, 2010] and the 21,739 cells sampled in the partial connectome of the *Drosophila* central brain [Scheffer *et al.*, 2020]. We found this number reasonable especially due to the nonuniformity found in primates that have no fixed number of neurons under 1 mm<sup>2</sup> of the cortex [Herculano-Houzel *et al.*, 2008] but that would have a higher density than any rodent of the same brain mass [Gabi *et al.*, 2010].

We hypothesized that both the selective death of neurons and the pruning of synapses would lead to significant changes in the topology of neuronal networks. Specifically, we expected these changes to enhance their robustness, reduce average path lengths and increase overall clustering. Our model builds upon fundamental assumptions derived from neurobiology: (1) neuronal death and synaptic pruning happen on a large scale during brain development, (2) their occurrence is selective, influenced by connectivity patterns, (3) neurons primarily access local connectivity information, and (4) the network exhibits a feed-forward structure with a preferred direction for most connections.

By combining these elements, we aim to provide insights into the interplay of brain development and network organization.

## 2 The model

### Definition of the Network

We model the network of neurons as graph  $G = (V, E)$ , where  $V$  is the set of neurons (vertices); and  $E$  is the set of synapses (edges). Connections between neurons are directed but binary - activity is not explicitly modelled. Time is discrete in the model. The evolution of the network over time is defined as follows:

- *Initial condition*: start with a network  $G$  with  $N_n$  ordered nodes and  $N_e$  randomly added edges, with the direction of each edge chosen independently according to the percentage of feed-forward edges;
- *Neuronal death stage (ND)*: For each node  $n$ , with probability  $D(n)$ , remove the node and all its edges. The probability  $D_n$  is calculated according to equation (1) (see below). After elimination, the same amount of nodes and edges removed is randomly added back to the network, restoring the number of nodes and edges to  $N_n$  and  $N_e$  at the end of each step.
- *Synaptic pruning stage (SP)*: For each existing edge  $E(i, j)$ , with probability  $P(i, j)$  (equation (2) below), remove the edge. Contrary to the neuronal death stage, no edges or nodes are added back to the network in this stage. The reasoning here is the longer duration of the synaptic pruning, which extends through adulthood in humans.

In the model, the ND stage represents the short post-natal period of intense cell death occurring in parallel with cortical neurogenesis, where the number of neurons goes through large variations but ends about the same after the process [Wong and Marín, 2019]. The SP stage represents the pruning of synapses in the course of development (through adulthood in humans, see [Nagappan-Chettiar *et al.*, 2023]).

Death and pruning probabilities are calculated as follows:

$$D(n) = A \exp \left( -k \frac{d_{IN}(n)N}{\sum_m d_{IN}(m)} \right) \quad (1)$$

$$P(i, j) = A \exp \left( -k \frac{d_{IN}(j)d_{OUT}(i)N^2}{\sum_m d_{IN}(m) \sum_m d_{OUT}(m)} \right) \quad (2)$$

where  $d_{IN}(n)$  and  $d_{OUT}(n)$  are, respectively, the incoming and outgoing degrees of node  $n$ ; and  $N$  is the number of nodes. The parameters  $A$  and  $k$  are used to regulate the rate of pruning in the simulations. The formula for neuronal death is thought to reflect activity-dependent survival; activity in a neuron is assumed to be approximately proportional to a number of incoming edges, through which the neuron would receive growth factors through anterograde transport [Tonra *et al.*, 1998, von Bartheld and Butowt, 2000]. In the case of synaptic pruning, we used the Hebbian learning mechanism of preserving the synapses which fire synchronously – to save computational costs, for an edge going from node  $i$  to node  $j$ , this is approximated by the product of the number of incoming edges of  $j$  and the number of outgoing edges of  $i$ .

Notice that the formulas take the degree of each node into account. This is the degree relative to the previous step, since degrees are altered by the removal of edges themselves, this could lead to a cascading effect if we used the updated values (i.e. a "hot" update). Nodes/edges are removed only after all probabilities are calculated.

Typically, in our simulations,  $N_n$  is 50,000 and  $N_e$  is 100,000 (Figure 1), and the number of iterations in the ND stage is set at 500. This was determined empirically: we noticed that after 500 iterations, the degree distribution seems stable. The number of iterations in the SP stage is determined naturally since the network is eventually destroyed by the removal of edges.

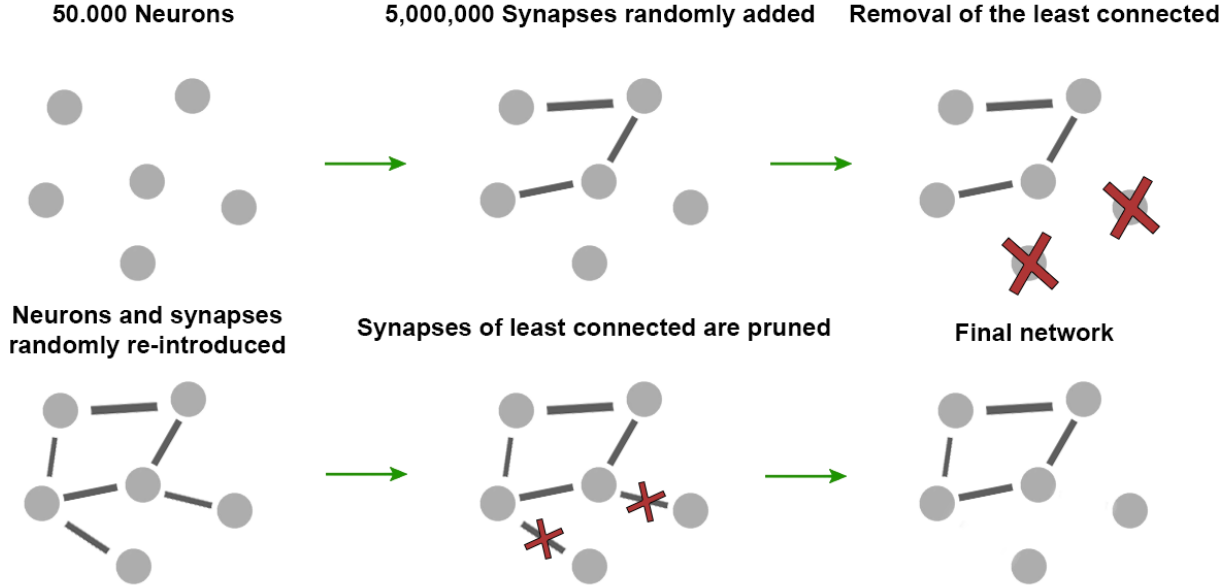


Figure 1: Main steps of our modular, evolving, and directed network graph.

### Implementation & Data Analysis

The model was implemented in Python 3 [Van Rossum et al., 1995], using the *igraph* [Csardi and Nepusz, 2006] and *SciPy* [Bressert, 2012] libraries. All posterior analysis and graphing were performed in Python, using *matplotlib* [Hunter, 2007] and *Seaborn* [Waskom et al., 2017]. The goodness of fit tests for the degree distributions was performed in accordance with the recommendations in [Clauset et al., 2009].

## 3 Results

The base model is generated using the criteria for neuronal death and synaptic pruning we chose *a priori* to resemble biological events of brain development (see Figure 1 in the Methods section for a detailed description).

We then compared the outputs of our model with a number of conditions. Namely, we wanted to measure the direct effects of the selective death and the selective pruning on the degree distributions after the model runs for the iterations needed for the ND and SP stages. First, we tested whether selective death is an essential factor. To test that, we ran the same simulation, the only change being the criteria for neuronal elimination in the death stage: we kept the same death rate as in the base model, but instead of the probability of death being inversely related to the degree, their dying probabilities were random. Furthermore, we performed a similar change for the probability of edges being pruned from the network.

### 3.1 Degree distributions

In figure 2 we show the degree distributions for our model as it progresses through its successive stages. During the neuronal death stage, the initial degree distribution converges to a combination of constant degree distribution for low degrees and a fat-tailed distribution for higher degrees

during the death stage starts with neurons of different degrees spread across the distribution and progresses towards a state where the rightmost portion of the distribution seems to have a heavy tail characteristic of power laws (Figure 2 - "Pruning" panel). Furthermore, our model (in blue) starts to show a more structured decline than the ones with random death (in orange). This distribution is stable (Figure 2 - "End" panel), up until the point where the number of neurons becomes too low. In Figure 2 - "End" panel, we see the cumulative degree distribution as the simulation continues to the pruning stage.

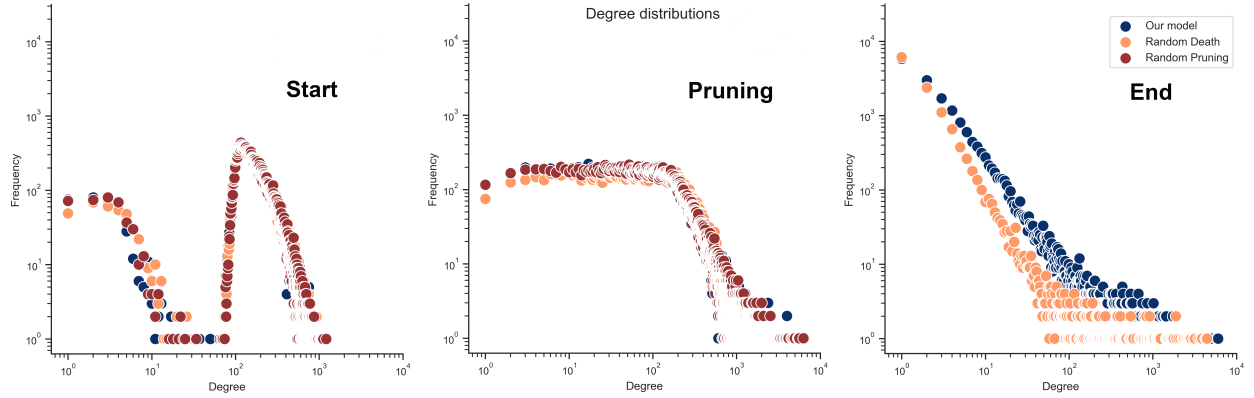


Figure 2: Distribution of the number of synapses (degree) of each neuron (node) in the network. The panels present the progression of the degree distribution in our model and colours stand for the different conditions tested, with blue being our base model with selective death and pruning, orange being when only the death is random and red when only the pruning is random.

We then evaluated if, as the iterations went on, the distributions progressed to a power-law distribution utilising the Kolmogorov-Smirnov test (K-S) [Cong *et al.*, 2020] test. The evolution of the exponent  $\alpha$  and the Kolmogorov-Smirnov distance  $D$  can be seen in figure 3. At iteration 5400 we have a  $D$  of 0.06 between the empirical distribution and a power law distribution with exponent 2.37. We took snapshots of the network and calculated the statistics for all 50 iterations of all of our generated networks. As the network evolves  $D$  gets smaller, pointing towards both our model and the network that was generated with random death being power laws ( $D = 0.06$ ,  $\alpha = 2.27$ , at 5400 iterations for the network generated with random death). The same cannot be said of the network generated with selective death and random pruning where the  $D$  varies in a less predictable fashion. Substituting the selective pruning for random pruning in the model makes the network slowly lose its edges randomly, thinning out until it is completely disconnected. It seems that not only a pruning stage, but a particular kind of pruning criteria is essential to generate the scale-free behaviour in the network model. The K-S test results clearly demonstrate that our model outperforms both random death and random pruning in maintaining a power-law distribution in the network.

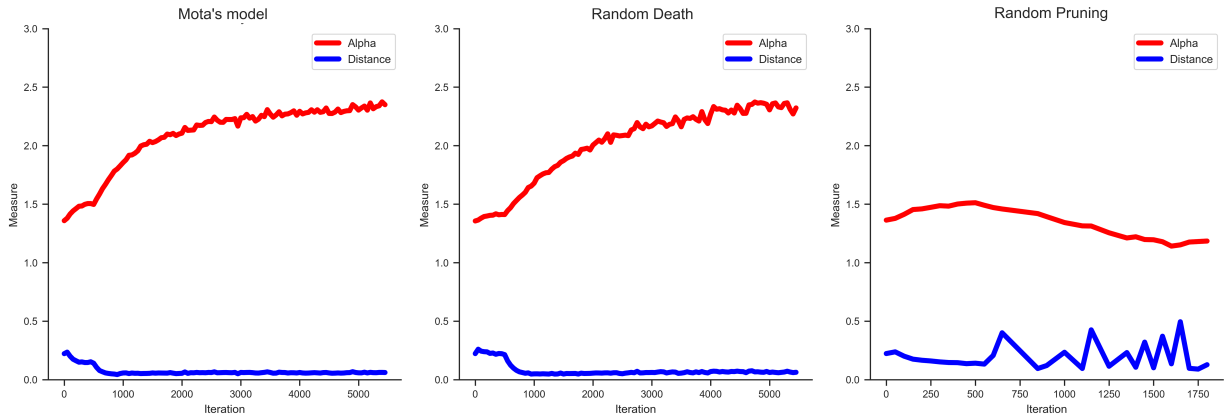


Figure 3: The evolution of the exponent  $\alpha$  and the Kolmogorov distance  $D$  as the simulation evolves.

### 3.2 Complex network statistics

When evaluating the complex network statistics of our model, we decided to also test different percentages of regulatory connections in the network. In other words, we varied the level of feed-forwardness of the network additionally. In Figure 4 we can see the evolution of the average shortest path length (ASPL), a measure that can be used as a proxy for

the efficiency of information or signal propagation within the network, providing insights into the overall connectivity and navigability of the network structure. During the death stage, all the ASPLs are constant at 2.86. However, during pruning, the ASPL is raised for around 500 iterations, especially in the network that has random pruning, where it gets to 6.41 only to decrease later in all networks but that one (the network with random pruning dies around 1500 iterations). By the end of the simulation, the ALSP returns to a lower level than before the pruning stage at 2.39 (2.52 if the death is random). Here, a critical ingredient seems to be the level of feed-forwardness of the network, apart from having a noticeably erratic behaviour throughout the simulation, for both 50% and 80% the ALSP is much higher than for the base model (100% of feed-forwardness) at 4.52 and 3.61, respectively. This points to a network that is harder to navigate as you add more regulatory connections.

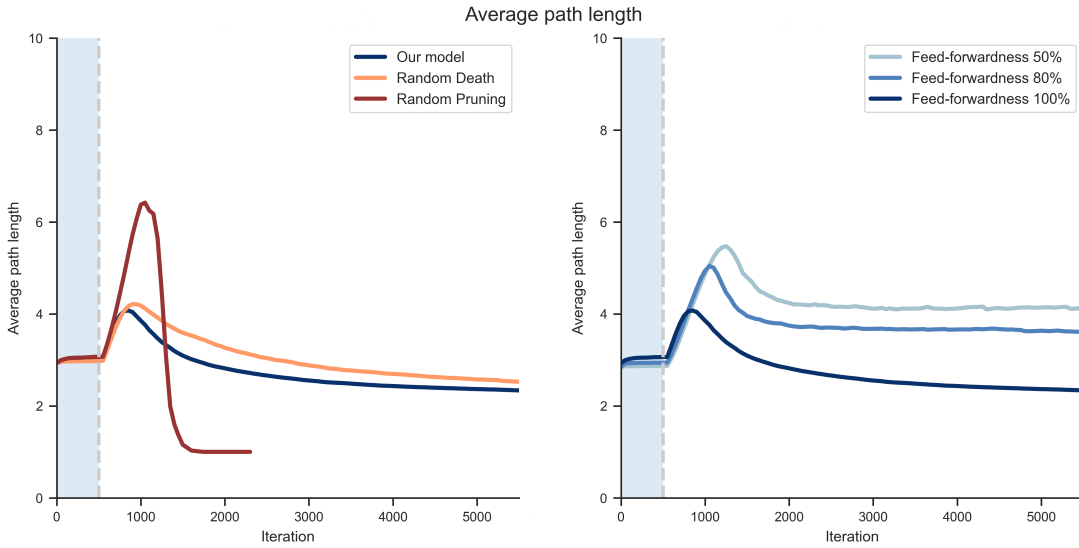


Figure 4: Evolution of the average path length in our model. (Left) Comparison with random death (orange) or random pruning (red). (Right) Various shades of blue indicate different degrees of feed-forwardness in the network, i.e. the percentage of regulatory connections. The shaded portion of the graph from 0 to 500 iterations represents the ND stage.

Brain networks are also expected to be cohesive and modular. To test this, we evaluated the clustering coefficient of all the network snapshots as time progressed in the simulations (Figure 5). Here, the key element seems to be the selective pruning once more, without which the network loses all cohesiveness by iteration 1500 (Figure 5, red in the left panel). For all other conditions, there is a sharp increase in the coefficient during the ND stage followed by a stabilisation phase. Notably, there is a marked delay in this stable phase for the lower levels of feed-forwardness (Figure 5, darker shade of blue in the right panel). This figure also shows a critical role for the selective death in the model, by the end of that stage the clustering coefficient is 0.021 if the death is random and 0.045 if it is performed selectively in the way we propose. Both networks seem to have a similar stabilisation stage during the pruning iterations ending up with a clustering coefficient of 0.11 if the death is random and 0.19 if it is selective. The role of the feed-forwardness in this stage is less pronounced, with a clustering coefficient of 0.14 for 50% and 0.18 for 80%, remarkably similar to our base model.

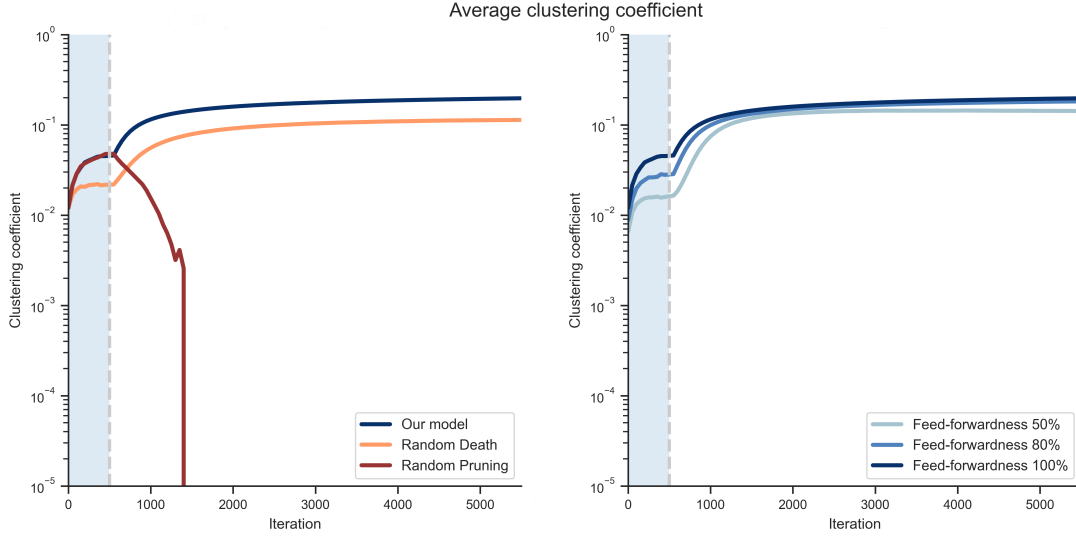


Figure 5: Evolution of the clustering coefficient in our model. (Left) Comparison with random death (orange) or random pruning (red). (Right) Various shades of blue indicate different degrees of feed-forwardness in the network, i.e. the percentage of regulatory connections. The shaded portion of the graph from 0 to 500 iterations represents the ND stage.

### 3.3 Synaptic preservation and pruning rates

The cohesive nature found in figure 5 led us to investigate the overall number of connections in the network when our hypothesis is followed (Figure 6). It is worth remembering that this is only possible in the SP stage since the synapses (edges) are re-introduced to the network during the ND stage. Markedly, the biologically-inspired model generates a more densely connected network than the alternatives tested and this seems to be directly proportional to the percentage of feed-forward connections in the network (Figure 6, right panel). By the end of the simulation, our model preserves 9.38% of the overall number of synapses versus only 2.32% if the death stage is performed randomly. This explains the increased clustering of our model in comparison to the simulations with random death. Furthermore, our model preserves almost double the number of connections when compared with the feed-forwardness set to 80%, where we have 4.17%, and if the feed-forwardness is set as 50% only 1% of the synapses remain in the network.



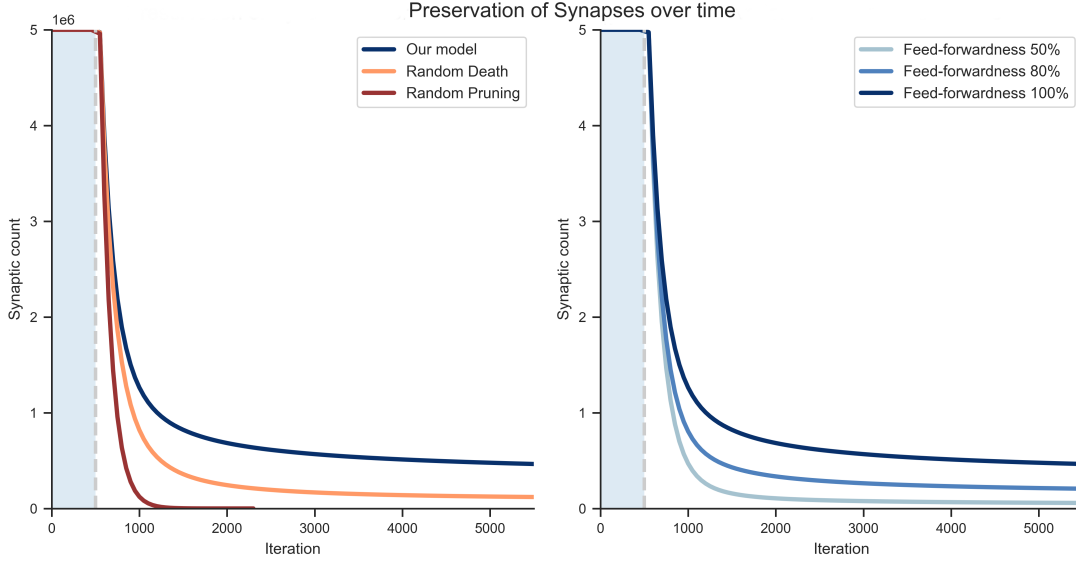


Figure 6: Number of synapses (edges) in the network as time progresses in the simulation. (Left) Comparison with random death (orange) or random pruning (red). (Right) Various shades of blue indicate different degrees of feed-forwardness in the network, i.e. the percentage of regulatory connections. The shaded portion of the graph from 0 to 500 iterations represents the ND stage.

Biological neuronal networks were recently found to have a decreasing pruning rate [Navlakha *et al.*, 2015]. This pattern is also found in our model and it is disrupted when the selective pruning is removed (Figure 7 - red in the left panel). The decrease in the pruning rate is also more pronounced in our model when compared to a network that went through a process of random death (Figure 7 - centre). This sharp decrease in the pruning rate repeats a pattern we found when testing other network statistics – it seems to be related to the percentage of regulatory connections in the network (Figure 7, right panel).

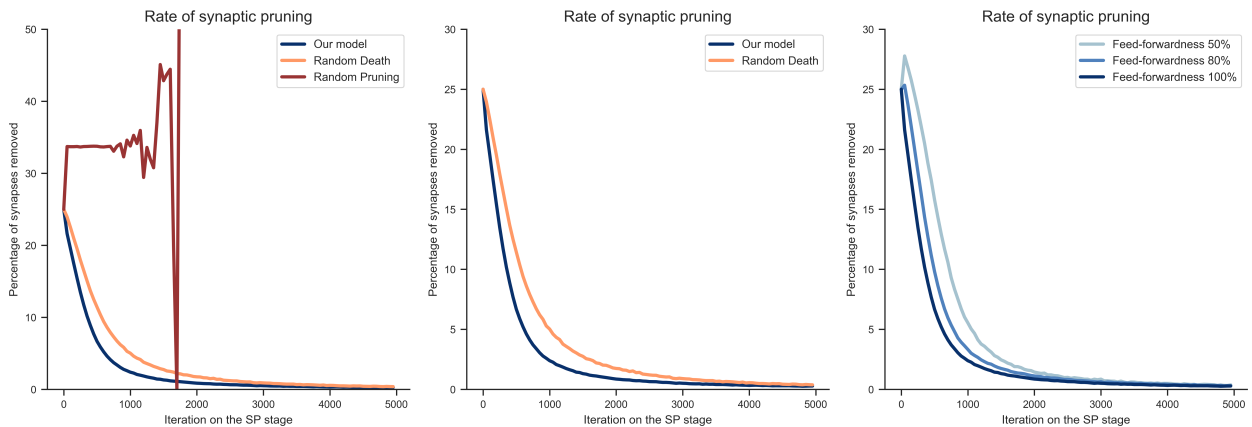


Figure 7: Percentage of connections (synapses) removed from the network per iteration of the simulation. (Left) Comparison with random death (orange) or random pruning (red). (Center) A closer look at the rates of synaptic pruning of the random death (orange) vs our model (blue). (Right) Various shades of blue indicate different degrees of feed-forwardness in the network, i.e. the percentage of regulatory connections.

### 3.4 Feed-forwardness

The aforementioned results established our main finding and base model: the biologically inspired dynamics we used to generate a network topology with signs of scale-invariance. Finally, we tested how the percentage of feed-forward synapses affects the evolution of network topology. In the base model, all edges are feed-forward. This is not the case in the cerebral cortex, where feedback and reciprocal connections are common enough such that the complete feed-forward assumption becomes unrealistic [Callaway, 1998, 2004]. Therefore, we test different percentages of feed-forwardness: 50% and 80%. We see that a certain amount of feed-forwardness is a requirement for the topology of the base model - the more, the closer it seems to the original power law, suggesting a causal role for feed-forwardness in the generation of the final network (**50%**:  $D = 0.07$ ,  $\alpha = 2.46$ ; **80%**:  $D = 0.06$ ,  $\alpha = 2.37$ ; **100%**:  $D = 0.06$ ,  $\alpha = 2.37$ , at 5400 iterations).

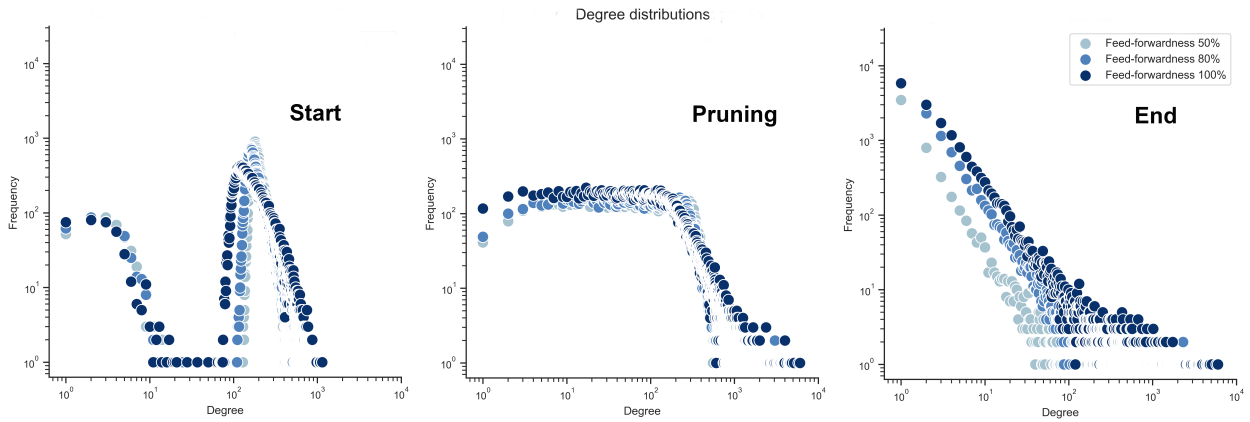


Figure 8: Distribution of the number of synapses (Degree) of each neuron (Node) in the network. The panels present the progression of the degree distribution in the three stages of our model and shades of blue represent for the different conditions tested, with blue representing different degrees of feed-forwardness in the network.

### 3.5 Sensitivity analysis of model parameters

The network development model discussed here, which draws inspiration from brain ontology, primarily revolves around two parameters:  $A$  and  $k$ , detailed in the Methods section (2). To assess the resilience and significance of these parameter values, we conducted a robustness test by significantly altering their absolute values. This experiment aimed to determine if minor variations in each parameter would trigger unforeseen model responses or if the model demonstrates adequate robustness to fluctuations in parameter settings. This approach also helps evaluate whether the relationship between the parameter values is crucial for the model to generate the scale-free degree distribution characteristic of heavy-tail connectivity.

The aforementioned degree distributions can be seen in figure 9. The parameter  $k$  appears robust to change (Figure 9 - Top row) except when lowered to an extreme level (0.01 vs the default 0.2) which, in turn, would render our pruning random and the network would run out of connections as shown in figure 2. Lower  $k$  values lead to a significant reduction in higher degree nodes, reflecting less selective, more aggressive pruning. Even more robust in terms of power-law generation is the parameter  $A$ . All options tested achieved a scale-free degree distribution by the end of the simulation (Figure 9 - Bottom row), in fact, for the higher end of the variation of  $A$  these distributions stabilised as a power law quicker than in the original model.

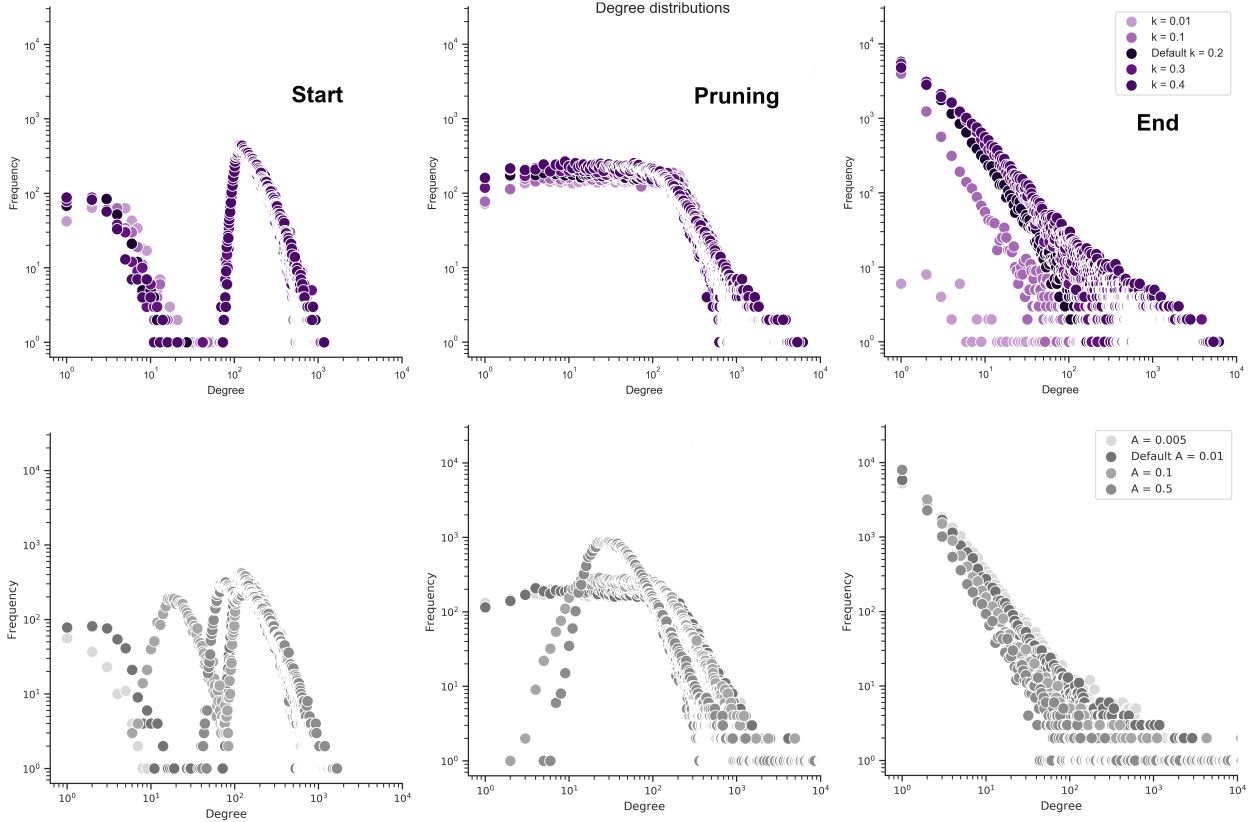


Figure 9: Distribution of the number of synapses (Degree) of each neuron (Node) in the network. The panels present the progression of the degree distribution in our model and shades of colour represent the different conditions tested, with purple representing different numbers of  $k$  and grey being used for the variation of  $A$ .

Furthermore, we investigated the effects that the jittering had on the complex network statistics (Figure 10). As in the base model case, the ASLP initially increases only to decrease. However, when reducing  $k$  to 0.01 we see different behaviour on the ASLP (Figure 10 - Top left panel) where it becomes quite unstable and does not converge to the same space as the other values, instead of keeping the final ASLP around 2.40 as the other values, it drops it to 1.23 which is consistent with the values found for the networks with random pruning tested against the base model (Figure 4). The changes in  $A$  seem to speed up the decrease of the ASLP to 2 and its stabilisation (Figure 10 - Top right panel), showing that  $A$  is more robust to jittering regarding ASLP than  $k$ . Similarly, the parameter  $A$  appears more robust to change than  $k$  when evaluating the clustering coefficient. For all tested values of  $k$ , the clustering coefficient first decreases to its lowest value of 0.01 to then increases to its maximum value of 0.46 to then stabilise at 0.28, slightly higher than the other values that group around 0.2. Finally, high values of the parameter  $A$  result in a quick stabilisation of the end values of the clustering coefficients.

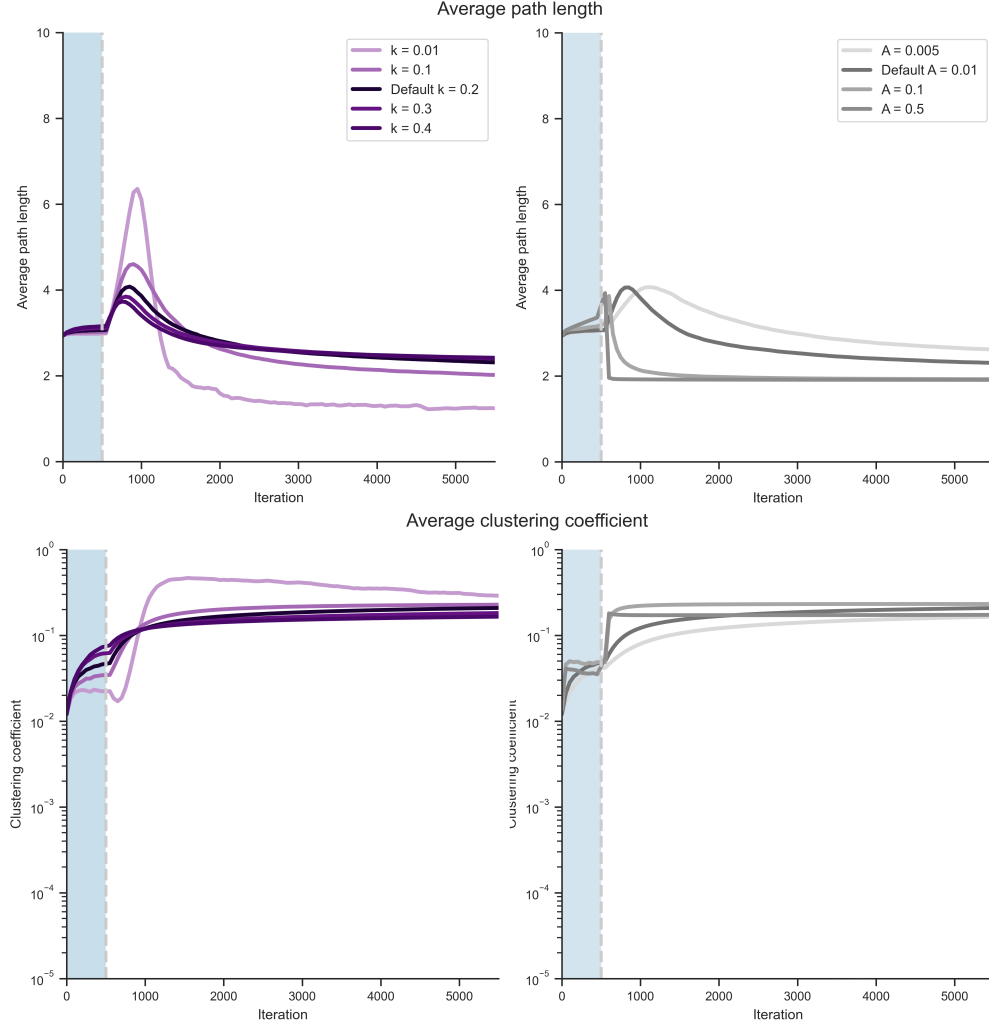


Figure 10: Evolution of the average path length (Top row) and clustering (Bottom row) in our model for different values of the parameters  $k$  and  $A$ . The panels present the progression of the degree distribution in our model and shades of colour represent the different conditions tested, with purple representing different numbers of  $k$  and grey being used for the variation of  $A$ .

## 4 Discussion

In this study, we utilised the framework provided by network neuroscience to devise a model that suggests that the destructive processes in the ontogeny of the nervous system can lead to heavy-tail connectivity in the form of a scale-invariant neuronal network, which could make it robust to random death of neurons by definition [Barabási, 2009]. This is not to say that these vastly destructive events were exclusively selected for this advantage. One possibility is that it is just a consequence of another necessary event that happens to provide a separate advantage, i.e. a spandrel [Gould and Lewontin, 1979]. For instance, neurogenesis is heavily concentrated at the beginning of brain development, leading to massive DNA replication errors and aneuploidy [McKinnon, 2013]. It could be that the massive apoptosis that follows is a corrective procedure, such that the cells with damaged DNA will not survive long.

Nevertheless, according to our theory, if neuronal death happens as a result of selective detachment, it could serve the purpose of priming the network before the major pruning events. In that way, it will prevent the over-pruning (Figure 16) that can lead not only to the implosion of the network but to known neurological conditions such as schizophrenia [Hong *et al.*, 2016b, Yilmaz *et al.*, 2021, Scott-Hewitt *et al.*, 2023]. Our model has two main parameters:  $A$ , which scales the overall probability of synaptic pruning and neuronal death, and  $k$  which regulates the exponential decay based on node connectivity (please refer to equations 1 and 2). The analysis indicates that the model is relatively robust to

jittering  $A$ , as all tested values resulted in a scale-free degree distribution by the end of the simulation. This suggests that the overall rate of pruning and death can vary without significantly disrupting the network's structural properties.

In contrast, the parameter  $k$  exhibits greater sensitivity. Lower values of  $k$  (e.g.,  $k=0.01$ ) lead to a more aggressive and less selective pruning process, resulting in a network that quickly loses its high-degree nodes and deviates from the desired scale-free structure. Higher values of  $k$  (e.g.,  $k=0.4$ ), however, maintain a more selective pruning process, preserving the network's integrity and resulting in a more stable power-law distribution. These findings pointed to  $k$  having been selected by evolution to ensure effective and selective pruning, according to our theory. It can be that neuronal death was a selected step in brain development that served the purpose of enabling maximum neuronal connectivity with the least amount of individual elements.

The shift in the power laws seen in the end panel of figure 2 could also be a consequence of the re-introduction of synapses during the death stage, this could generate some variability in the degree distribution that will go through the pruning stage. In fact, since neuronal death does not seem essential to the model's scale-free behaviour, it would warrant another explanation. One possibility is brought by the results shown in figures 15 and 16. When neuronal death does not happen selectively, the rate of pruning does not drop optimally, resulting in fewer synapses preserved in the network. Random removal of neurons pushes the initial pruning rate to higher values, leading to a more pronounced reduction in the number of synapses. A similar case of over-pruning is, indeed, seen in schizophrenia [Yilmaz *et al.*, 2021]. Conversely, networks generated with random death will still moderately preserve local clustering and connectivity.

Thus, selective synaptic pruning is our essential ingredient and is a direct consequence of learning [Ma *et al.*, 2020, Scholl *et al.*, 2021]. A recent study measured synaptic loss over time using electronic microscopy images [Navlakha *et al.*, 2015]. Our model of selective detachment generates the same pattern of decreasing pruning rates (Figure 16). The same study showed that removing edges is an effective way of indirectly designing efficient networks for any purpose [Navlakha *et al.*, 2015], lending support to the idea that this is a useful feature for a neuronal network. Our results show that if the reduction of synaptic numbers is performed in a random way, it will result in an unstable and aggressive synaptic removal stage that will quickly decrease the number of connections in the network. Our model seems to produce a controlled and efficient pruning process that maintains network stability preserving local clustering and reducing the ALSP.

The heavy-tail connectivity presented also would be of behavioural importance as it was recently found in functional connectivity studies [Kardan *et al.*, 2023]. Kardan *et al.* showed that more efficient information processing during a cognitive task may be indicated by higher fMRI scale-free activity, and this could predict further improvements in task performance [Kardan *et al.*, 2023]. In terms of complex network statistics, our findings seem to be in line with functional connectivity studies [Van Den Heuvel *et al.*, 2009].

Beyond the neurobiological inspirations of the model, it has not escaped our notice that our results have consequences for the theoretical understanding of scale-free networks more generally. Our work suggests that scale-free networks can be generated by a selective deletion mechanism. Previously, all other network models shown to have this characteristic relied on some form of selective attachment [Hébert-Dufresne *et al.*, 2011, Bell *et al.*, 2017]. This is, to our knowledge, only the second class of algorithms that generate scale-free networks, the other being the Barabási-Albert/Barabási-Bianconi class of models [Barabási and Albert, 1999, Bianconi and Barabási, 2001]. While reaching the same scale-free distribution, the algorithms differ in one main aspect: our model is preferential in the deletion of edges while the Barabási-Bianconi model is preferential in the addition of nodes and edges.

The underlying similarities are more interesting, however, as they might suggest a general principle. Taking the simpler Barabási-Albert model as an example, it applies *preferential addition of edges* on top of a *temporal inequality* - older nodes are preferred since they will have spent more iterations able to receive new edges and will likely have accumulated more edges in the course of the simulation. Our model has one required ingredient: selective elimination of edges. However, the resulting network seems more robust when it starts from feed-forward connectivity. This is analogous to the Barabási-Albert model, in the sense that our model applies *preferential deletion of edges* on top of a *spatial inequality*: in a feed-forward network, nodes at the end of the network can receive edges originating in any of the nodes behind it, while nodes at the beginning of the network cannot. As a consequence, end nodes will likely have a higher degree from the beginning.

The possible mechanisms, then, might include not only "richer-gets-richer", as in the Barabási-Bianconi model, but also "poorer-gets-poorer", as in our model. More synthetically, an existing inequality is reinforced by a process: inequality upon inequality. We have scale-free networks more easily when an algorithm that is degree-dependent is applied to a structure that already contains an underlying inequality in degree distribution (temporal or spatial). It remains to be explored how much the particular form of the unequal distribution or the shape of the detachment mechanism matters.

For both deletion and attachment, the various possible definitions of selectiveness define whole classes of models. Presently, we have used a simplified measure of connectivity as a selection function; it is relatively straightforward to

incorporate into this function more complex algebraic quantifications of connectivity, as well as wiring and metabolic costs. Alternatively, if one includes any class of simulated spiking activity into the networks, one can preferentially delete neurons/synapses that are the most task- or representation-irrelevant. Indeed, a version of this mechanism has been shown to overcome catastrophic forgetting in artificial networks [Peng *et al.*, 2021]. Additionally, scale-free structural connectivity was already demonstrated in the mouse visual cortex’s response to natural images when considering the distribution of activity covariances [Stringer *et al.*, 2019]. We intend to explore all these alternative implementations of selectiveness in the future. Again, we stress that we are not attempting to simulate cortical development in detail here. Rather, we show that mechanisms and structures known to exist in the developing cortical are sufficient to generate scale-free networks with the characteristics listed above robustly. For now, it was worthwhile to show that scale-invariance can arise in feed-forward networks from the simplest possible version of the selective deletion mechanism.

## Acknowledgements

The authors would like to thank our dear friend Roberto Marinho who sadly could not see this work all the way to its publication. We would also like to thank Dr Jon Stammers at the AMRC for encouraging Rodrigo’s pursuit of his ideas and Dr Hannes Saal at the Active Touch Lab for allowing us to run the simulation and analysis at his group’s HPC. We also thank Suzana Herculano-Houzel for the fruitful discussions in the conception of this project. Francesca Redmore and the metaBIO team also deserve thanks for the help with proofreading.

## Data and code availability

Data from the model simulations are available at Zenodo. All code for the model and analysis is available on GitHub.

## References

- Maja Abitz, Rune Damgaard Nielsen, Edward G Jones, Henning Laursen, Niels Graem, and Bente Pakkenberg. Excess of neurons in the human newborn mediodorsal thalamus compared with that of the adult. *Cerebral Cortex*, 17(11): 2573–2578, 2007.
- Zdravko Petanjek, Miloš Judaš, Goran Šimić, Mladen Roko Rašin, Harry BM Uylings, Pasko Rakic, and Ivica Kostović. Extraordinary neoteny of synaptic spines in the human prefrontal cortex. *Proceedings of the National Academy of Sciences*, 108(32):13281–13286, 2011.
- Viktor Hamburger, Viktor Hamburger, and Ronald W Oppenheim. Naturally occurring neuronal death in vertebrates. *Neuroembryology: The Selected Papers*, pages 126–142, 1990.
- Jean-Pierre Changeux and Antoine Danchin. Selective stabilisation of developing synapses as a mechanism for the specification of neuronal networks. *Nature*, 264(5588):705, 1976.
- Fabiana Bandeira, Roberto Lent, and Suzana Herculano-Houzel. Changing numbers of neuronal and non-neuronal cells underlie postnatal brain growth in the rat. *Proceedings of the National Academy of Sciences*, 106(33):14108–14113, 2009.
- PGH Clarke. Neuronal death in the development of the vertebrate nervous system. *Trends in Neurosciences*, 8:345–349, 1985.
- Tarik F Haydar, Chia-Yi Kuan, Richard A Flavell, and Pasko Rakic. The role of cell death in regulating the size and shape of the mammalian forebrain. *Cerebral Cortex*, 9(6):621–626, 1999.
- Peter R Huttenlocher *et al.* Synaptic density in human frontal cortex—developmental changes and effects of aging. *Brain Res*, 163(2):195–205, 1979.
- Joan Stiles and Terry L Jernigan. The basics of brain development. *Neuropsychology review*, 20(4):327–348, 2010.
- Guy N Elston, Tomofumi Oga, and Ichiro Fujita. Spinogenesis and pruning scales across functional hierarchies. *Journal of Neuroscience*, 29(10):3271–3275, 2009.
- Fergus IM Craik and Ellen Bialystok. Cognition through the lifespan: mechanisms of change. *Trends in cognitive sciences*, 10(3):131–138, 2006.
- William D Snider, Jeffrey L Elliott, and Qiao Yan. Axotomy-induced neuronal death during development. *Developmental Neurobiology*, 23(9):1231–1246, 1992.
- Rosa C Paolicelli, Giulia Bolasco, Francesca Pagani, Laura Maggi, Maria Scianni, Patrizia Panzanelli, Maurizio Giustetto, Tiago Alves Ferreira, Eva Guiducci, Laura Dumas, *et al.* Synaptic pruning by microglia is necessary for normal brain development. *science*, 333(6048):1456–1458, 2011.

- Hiroaki Wake, Andrew J Moorhouse, Shozo Jinno, Shinichi Kohsaka, and Junichi Nabekura. Resting microglia directly monitor the functional state of synapses in vivo and determine the fate of ischemic terminals. *Journal of Neuroscience*, 29(13):3974–3980, 2009.
- Dorothy P Schafer, Emily K Lehrman, Amanda G Kautzman, Ryuta Koyama, Alan R Mardinly, Ryo Yamasaki, Richard M Ransohoff, Michael E Greenberg, Ben A Barres, and Beth Stevens. Microglia sculpt postnatal neural circuits in an activity and complement-dependent manner. *Neuron*, 74(4):691–705, 2012.
- Michael SC Thomas, Rachael Davis, Annette Karmiloff-Smith, Victoria CP Knowland, and Tony Charman. The over-pruning hypothesis of autism. *Developmental science*, 19(2):284–305, 2016.
- Olivia M Teter, Nina M Draeger, Sydney M Sattler, Amanda McQuade, Brandon B Holmes, Vasileios Papakis, Kun Leng, Steven Boggess, David Shin, Tomasz J Nowakowski, et al. Crispri-based screen of autism spectrum disorder risk genes in microglia uncovers roles of adnp in microglia endocytosis and uptake of synaptic material. *bioRxiv*, pages 2024–06, 2024.
- Allison M Rosen and Beth Stevens. The role of the classical complement cascade in synapse loss during development and glaucoma. *Inflammation and Retinal Disease: Complement Biology and Pathology*, pages 75–93, 2010.
- Gareth R Howell, Danilo G Macalinao, Gregory L Sousa, Michael Walden, Ileana Soto, Stephen C Kneeland, Jessica M Barbay, Benjamin L King, Jeffrey K Marchant, Matthew Hibbs, et al. Molecular clustering identifies complement and endothelin induction as early events in a mouse model of glaucoma. *The Journal of clinical investigation*, 121(4):1429–1444, 2011.
- Daniel K Wilton, Kevin Mastro, Molly D Heller, Frederick W Gergits, Carly Rose Willing, Jaclyn B Fahey, Arnaud Frouin, Anthony Daggett, Xiaofeng Gu, Yejin A Kim, et al. Microglia and complement mediate early corticostriatal synapse loss and cognitive dysfunction in huntington’s disease. *Nature Medicine*, 29(11):2866–2884, 2023.
- Melis Yilmaz, Esra Yalcin, Jessy Presumey, Ernest Aw, Minghe Ma, Christopher W Whelan, Beth Stevens, Steven A McCarroll, and Michael C Carroll. Overexpression of schizophrenia susceptibility factor human complement c4a promotes excessive synaptic loss and behavioral changes in mice. *Nature neuroscience*, 24(2):214–224, 2021.
- Soyon Hong, Victoria F Beja-Glasser, Bianca M Nfonoyim, Arnaud Frouin, Shaomin Li, Saranya Ramakrishnan, Katherine M Merry, Qiaoqiao Shi, Arnon Rosenthal, Ben A Barres, et al. Complement and microglia mediate early synapse loss in alzheimer mouse models. *Science*, 352(6286):712–716, 2016a.
- Hansen Lui, Jiasheng Zhang, Stefanie R Makinson, Michelle K Cahill, Kevin W Kelley, Hsin-Yi Huang, Yulei Shang, Michael C Oldham, Lauren Herl Martens, Fuying Gao, et al. Progranulin deficiency promotes circuit-specific synaptic pruning by microglia via complement activation. *Cell*, 165(4):921–935, 2016.
- Soyon Hong, Lasse Dissing-Olesen, and Beth Stevens. New insights on the role of microglia in synaptic pruning in health and disease. *Current opinion in neurobiology*, 36:128–134, 2016b.
- Nicole Scott-Hewitt, Youtong Huang, and Beth Stevens. Convergent mechanisms of microglia-mediated synaptic dysfunction contribute to diverse neuropathological conditions. *Annals of the New York Academy of Sciences*, 1525(1):5–27, 2023.
- Donald O Hebb et al. The organization of behavior: A neuropsychological theory, 1949.
- Natalia Bastrikova, Gregory A Gardner, Jeff M Reece, Andreas Jeromin, and Serena M Dudek. Synapse elimination accompanies functional plasticity in hippocampal neurons. *Proceedings of the National Academy of Sciences*, 105(8):3123–3127, 2008.
- Qiang Zhou, Koichi J Homma, and Mu-ming Poo. Shrinkage of dendritic spines associated with long-term depression of hippocampal synapses. *Neuron*, 44(5):749–757, 2004.
- Daniel A Butts, Patrick O Kanold, and Carla J Shatz. A burst-based “hebbian” learning rule at retinogeniculate synapses links retinal waves to activity-dependent refinement. *PLoS biology*, 5(3):e61, 2007.
- Jiayi Zhang, James B Ackman, Hong-Ping Xu, and Michael C Crair. Visual map development depends on the temporal pattern of binocular activity in mice. *Nature neuroscience*, 15(2):298, 2012.
- Anirvan Ghosh, Josette Carnahan, and Michael E Greenberg. Requirement for bdnf in activity-dependent survival of cortical neurons. *Science*, 263(5153):1618–1623, 1994.
- Suzanaerculano-Houzel. The human brain in numbers: a linearly scaled-up primate brain. *Frontiers in human neuroscience*, page 31, 2009.
- Ashish Raj and Yu-hsien Chen. The wiring economy principle: connectivity determines anatomy in the human brain. *PloS one*, 6(9):e14832, 2011.
- Danielle S Bassett and Olaf Sporns. Network neuroscience. *Nature neuroscience*, 20(3):353–364, 2017.

- Ed Bullmore and Olaf Sporns. Complex brain networks: graph theoretical analysis of structural and functional systems. *Nature reviews neuroscience*, 10(3):186–198, 2009.
- Danielle S Bassett and Edward T Bullmore. Small-world brain networks revisited. *The Neuroscientist*, 23(5):499–516, 2017.
- Martijn P Van den Heuvel, Edward T Bullmore, and Olaf Sporns. Comparative connectomics. *Trends in cognitive sciences*, 20(5):345–361, 2016.
- Maria Grazia Puxeddu, Joshua Faskowitz, Richard F Betzel, Manuela Petti, Laura Astolfi, and Olaf Sporns. The modular organization of brain cortical connectivity across the human lifespan. *NeuroImage*, 218:116974, 2020.
- Nicolas A Crossley, Andrea Mechelli, Jessica Scott, Francesco Carletti, Peter T Fox, Philip McGuire, and Edward T Bullmore. The hubs of the human connectome are generally implicated in the anatomy of brain disorders. *Brain*, 137(8):2382–2395, 2014.
- Martijn P Van Den Heuvel and Olaf Sporns. Rich-club organization of the human connectome. *Journal of Neuroscience*, 31(44):15775–15786, 2011.
- Matthew L Stanley, Malaak N Moussa, Brielle M Paolini, Robert G Lyday, Jonathan H Burdette, and Paul J Laurienti. Defining nodes in complex brain networks. *Frontiers in computational neuroscience*, 7:169, 2013.
- Moritz Helmstaedter. Cellular-resolution connectomics: challenges of dense neural circuit reconstruction. *Nature methods*, 10(6):501–507, 2013.
- Louis K Scheffer, C Shan Xu, Michal Januszewski, Zhiyuan Lu, Shin-ya Takemura, Kenneth J Hayworth, Gary B Huang, Kazunori Shinomiya, Jeremy Maitlin-Shepard, Stuart Berg, et al. A connectome and analysis of the adult drosophila central brain. *elife*, 9:e57443, 2020.
- Shin-ya Takemura, Arjun Bharioke, Zhiyuan Lu, Aljoscha Nern, Shiv Vitaladevuni, Patricia K Rivlin, William T Katz, Donald J Olbris, Stephen M Plaza, Philip Winston, et al. A visual motion detection circuit suggested by drosophila connectomics. *Nature*, 500(7461):175–181, 2013.
- John G White, Eileen Southgate, J Nichol Thomson, Sydney Brenner, et al. The structure of the nervous system of the nematode *caenorhabditis elegans*. *Philos Trans R Soc Lond B Biol Sci*, 314(1165):1–340, 1986.
- Emma K Towlson, Petra E Vértes, Sebastian E Ahnert, William R Schafer, and Edward T Bullmore. The rich club of the *c. elegans* neuronal connectome. *Journal of Neuroscience*, 33(15):6380–6387, 2013.
- Nadine Randel, Albina Asadulina, Luis A Bezares-Calderón, Csaba Verasztó, Elizabeth A Williams, Markus Conzelmann, Réza Shahidi, and Gáspár Jékely. Neuronal connectome of a sensory-motor circuit for visual navigation. *elife*, 3:e02730, 2014.
- Christopher W Lynn, Caroline M Holmes, and Stephanie E Palmer. Heavy-tailed neuronal connectivity arises from hebbian self-organization. *Nature Physics*, pages 1–8, 2024.
- Carsen Stringer, Marius Pachitariu, Nicholas Steinmetz, Matteo Carandini, and Kenneth D Harris. High-dimensional geometry of population responses in visual cortex. *Nature*, 571(7765):361–365, 2019.
- Albert-László Barabási. Scale-free networks: a decade and beyond. *science*, 325(5939):412–413, 2009.
- Priscilla Morterá and Suzana Herculano-Houzel. Age-related neuronal loss in the rat brain starts at the end of adolescence. *Frontiers in neuroanatomy*, 6:45, 2012.
- Albert-László Barabási and Réka Albert. Emergence of scaling in random networks. *science*, 286(5439):509–512, 1999.
- Ginestra Bianconi and A-L Barabási. Competition and multiscaling in evolving networks. *EPL (Europhysics Letters)*, 54(4):436, 2001.
- Michael Bell, Supun Perera, Mahendrarajah Piraveenan, Michiel Bliemer, Tanya Latty, and Chris Reid. Network growth models: A behavioural basis for attachment proportional to fitness. *Scientific reports*, 7(1):1–11, 2017.
- Vincenzo Nicosia, Takuya Machida, Richard Wilson, Edwin Hancock, Norio Konno, Vito Latora, and Simone Severini. Co-evolution of networks and quantum dynamics: a generalization of preferential attachment. *Journal of Statistical Mechanics: Theory and Experiment*, 2013(08):P08016, 2013.
- Rodney J Douglas, Kevan AC Martin, and David Whitteridge. A canonical microcircuit for neocortex. *Neural computation*, 1(4):480–488, 1989.
- Hanno S Meyer, Verena C Wimmer, Marcel Oberlaender, Christiaan PJ De Kock, Bert Sakmann, and Moritz Helmstaedter. Number and laminar distribution of neurons in a thalamocortical projection column of rat vibrissal cortex. *Cerebral cortex*, 20(10):2277–2286, 2010.



- Suzanaerculano-Houzel, Christine E Collins, Peiyan Wong, Jon H Kaas, and Roberto Lent. The basic nonuniformity of the cerebral cortex. *Proceedings of the National Academy of Sciences*, 105(34):12593–12598, 2008.
- Mariana Gabi, Christine E Collins, Peiyan Wong, Laila B Torres, Jon H Kaas, and Suzana Herculano-Houzel. Cellular scaling rules for the brains of an extended number of primate species. *Brain Behavior and Evolution*, 76(1):32–44, 2010.
- Fong Kuan Wong and Oscar Marín. Developmental cell death in the cerebral cortex. *Annual review of cell and developmental biology*, 35:523–542, 2019.
- Sivapratha Nagappan-Chettiar, Masahiro Yasuda, Erin M Johnson-Venkatesh, and Hisashi Umemori. The molecular signals that regulate activity-dependent synapse refinement in the brain. *Current Opinion in Neurobiology*, 79:102692, 2023.
- James R Tonra, Rory Curtis, Vivien Wong, Kenneth D Cliffer, John S Park, Andrew Timmes, Trang Nguyen, Ronald M Lindsay, Ann Acheson, and Peter S DiStefano. Axotomy upregulates the anterograde transport and expression of brain-derived neurotrophic factor by sensory neurons. *Journal of Neuroscience*, 18(11):4374–4383, 1998.
- Christopher S von Bartheld and Rafal Butowt. Expression of neurotrophin-3 (nt-3) and anterograde axonal transport of endogenous nt-3 by retinal ganglion cells in chick embryos. *Journal of Neuroscience*, 20(2):736–748, 2000.
- Guido Van Rossum, Fred L Drake, et al. *Python reference manual*, volume 111. Centrum voor Wiskunde en Informatica Amsterdam, 1995.
- Gabor Csardi and Tamas Nepusz. The igraph software package for complex network research. *InterJournal, Complex Systems*, 1695(5):1–9, 2006.
- Eli Bressert. Scipy and numpy: an overview for developers. 2012.
- J. D. Hunter. Matplotlib: A 2d graphics environment. *Computing In Science & Engineering*, 9(3):90–95, 2007. doi:10.1109/MCSE.2007.55.
- Michael Waskom, Olga Botvinnik, Drew O’Kane, Paul Hobson, Saulius Lukauskas, David C Gemperline, Tom Augspurger, Yaroslav Halchenko, John B. Cole, Jordi Warmenhoven, Julian De Ruiter, Cameron Pye, Stephan Hoyer, Jake Vanderplas, Santi Villalba, Gero Kunter, Eric Quintero, Pete Bachant, Marcel Martin, Kyle Meyer, Alistair Miles, Yoav Ram, Tal Yarkoni, Mike Lee Williams, Constantine Evans, Clark Fitzgerald, , Brian, Chris Fonnesbeck, Antony Lee, and Adel Qalieh. mwaskom/seaborn: v0.8.1 (september 2017), 2017.
- Aaron Clauset, Cosma Rohilla Shalizi, and Mark EJ Newman. Power-law distributions in empirical data. *SIAM review*, 51(4):661–703, 2009.
- Zicun Cong, Lingyang Chu, Yu Yang, and Jian Pei. Comprehensible counterfactual explanation on kolmogorov-smirnov test. *arXiv preprint arXiv:2011.01223*, 2020.
- Saket Navlakha, Alison L Barth, and Ziv Bar-Joseph. Decreasing-rate pruning optimizes the construction of efficient and robust distributed networks. *PLoS computational biology*, 11(7):e1004347, 2015.
- Edward M Callaway. Local circuits in primary visual cortex of the macaque monkey. *Annual review of neuroscience*, 21(1):47–74, 1998.
- Edward M Callaway. Feedforward, feedback and inhibitory connections in primate visual cortex. *Neural Networks*, 17(5-6):625–632, 2004.
- Stephen Jay Gould and Richard C Lewontin. The spandrels of san marco and the panglossian paradigm: a critique of the adaptationist programme. *Proc. R. Soc. Lond. B*, 205(1161):581–598, 1979.
- Peter J McKinnon. Maintaining genome stability in the nervous system. *Nature neuroscience*, 16(11):1523–1529, 2013.
- Xiaokuang Ma, Ke Chen, Yuehua Cui, Guanqun Huang, Antoine Nehme, Le Zhang, Handong Li, Jing Wei, Katerina Liong, Qiang Liu, et al. Depletion of microglia in developing cortical circuits reveals its critical role in glutamatergic synapse development, functional connectivity, and critical period plasticity. *Journal of Neuroscience Research*, 98(10):1968–1986, 2020.
- Carolin Scholl, Michael E Rule, and Matthias H Hennig. The information theory of developmental pruning: Optimizing global network architectures using local synaptic rules. *PLoS Computational Biology*, 17(10):e1009458, 2021.
- Omid Kardan, Andrew J Stier, Elliot A Layden, Kyoung Whan Choe, Muxuan Lyu, Xihan Zhang, Sian L Beilock, Monica D Rosenberg, and Marc G Berman. Improvements in task performance after practice are associated with scale-free dynamics of brain activity. *Network Neuroscience*, pages 1–63, 2023.
- Martijn P Van Den Heuvel, Cornelis J Stam, René S Kahn, and Hilleke E Hulshoff Pol. Efficiency of functional brain networks and intellectual performance. *Journal of Neuroscience*, 29(23):7619–7624, 2009.

Laurent Hébert-Dufresne, Antoine Allard, Vincent Marceau, Pierre-André Noël, and Louis J Dubé. Structural preferential attachment: Network organization beyond the link. *Physical review letters*, 107(15):158702, 2011.

Jian Peng, Bo Tang, Hao Jiang, Zhuo Li, Yinjie Lei, Tao Lin, and Haifeng Li. Overcoming long-term catastrophic forgetting through adversarial neural pruning and synaptic consolidation. *IEEE Transactions on Neural Networks and Learning Systems*, 33(9):4243–4256, 2021.

## Appendix: Sparse Networks

This appendix explores the structure of sparse neural networks with respect to scale-free properties. That is, we studied networks having 10 synapses on average per neuron, which results in a total of 500,000 connections, significantly less dense than the five million synapses that were analysed in the main findings section. Besides, these simulations have an overall 3000 iterations in opposition to the main text, which runs for 5500 for the network as the network is pruned 5000 times.

Figure 11 shows degree distributions revealing heavy-tailed features after selective death and pruning (blue) (K-S test can be seen in figure 12). This is different from what happens during random neuronal death (orange) or after random synaptic pruning (red), which are also not well organized but don't exhibit power-law characteristics. Therefore, even when densities reduce for sparser structures, specific mechanisms used to prune must be retained to maintain scale-free topology.

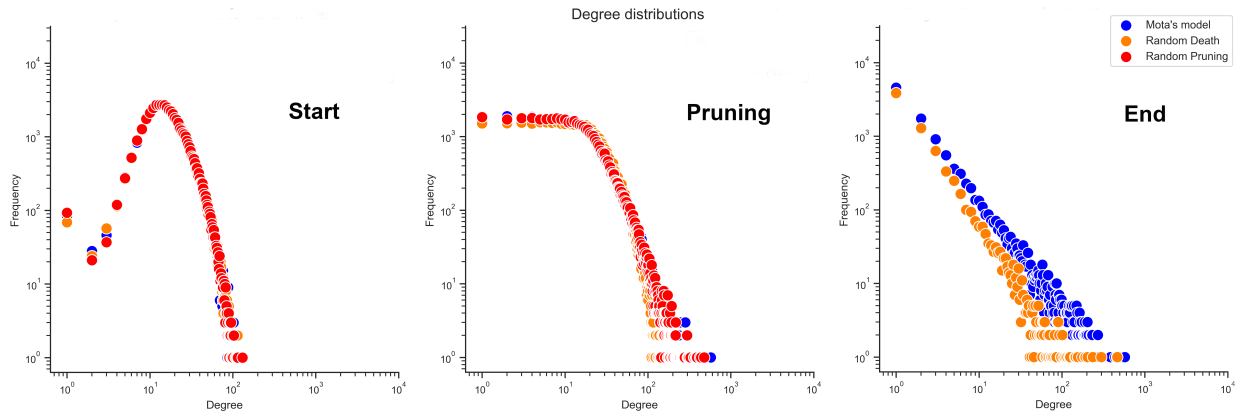


Figure 11: Distribution of the number of synapses (degree) of each neuron (node) in the network. The panels present the progression of the degree distribution in our model and colours stand for the different conditions tested, with blue being our base model with selective death and pruning, orange being when only the death is random and red when only the pruning is random.

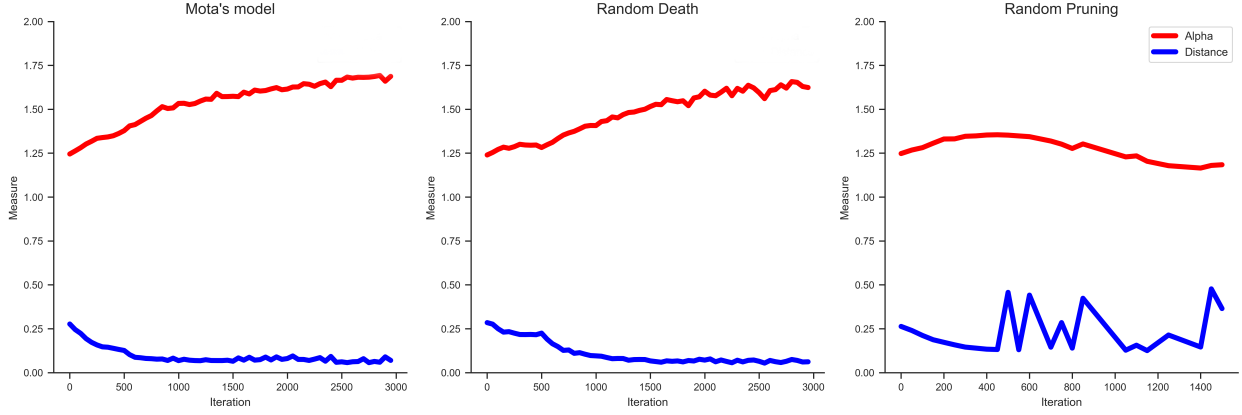


Figure 12: The evolution of the exponent alpha and the Kolmogorov distance  $D$  as the simulation evolves.

Figures 12 – 17 illustrate the evolution of network metrics over time. The K-S distance and power-law exponent (Figure 12) indicate that the network increasingly obeys power-law distribution. At 2350 iterations, for instance, the K-S distance ( $D$ ) is measured at 0.059 with an alpha exponent equal to 1.693 which is indicative of a stable power-law distribution. Average path length (Figure 13) and clustering coefficient (Figure 14) show that selective pruning maintains network efficiency and cohesiveness, whereas random pruning disrupts these properties. Figure 15 illustrates the number of synapses preserved whilst the pruning rates are shown in figure 16. A high number of feed-forward connections in networks ensures more controlled and steady pruning when compared to low feed-forward connection networks that lead to the maintenance of functionality as well as structure.

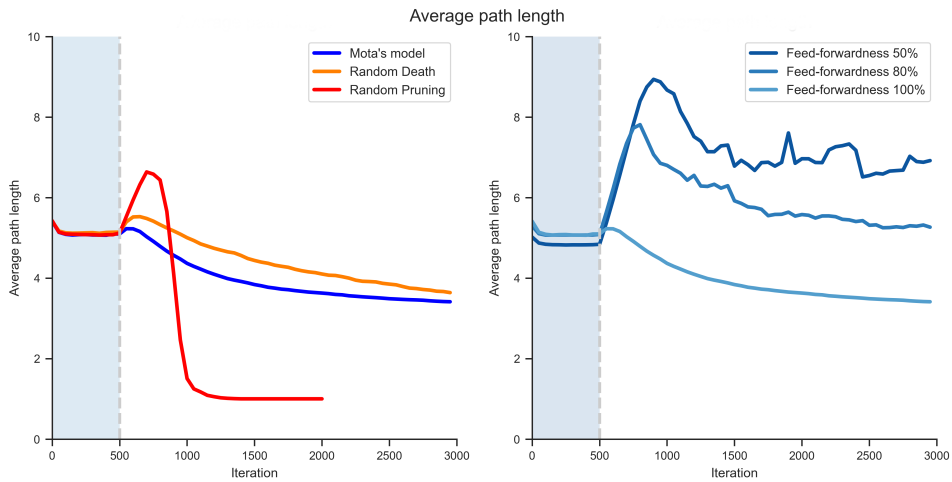


Figure 13: Evolution of the average path length in our model. (Left) Comparison with random death (orange) or random pruning (red). (Right) Various shades of blue indicate different degrees of feed-forwardness in the network, i.e. the percentage of regulatory connections. The shaded portion of the graph from 0 to 500 iterations represents the ND stage.

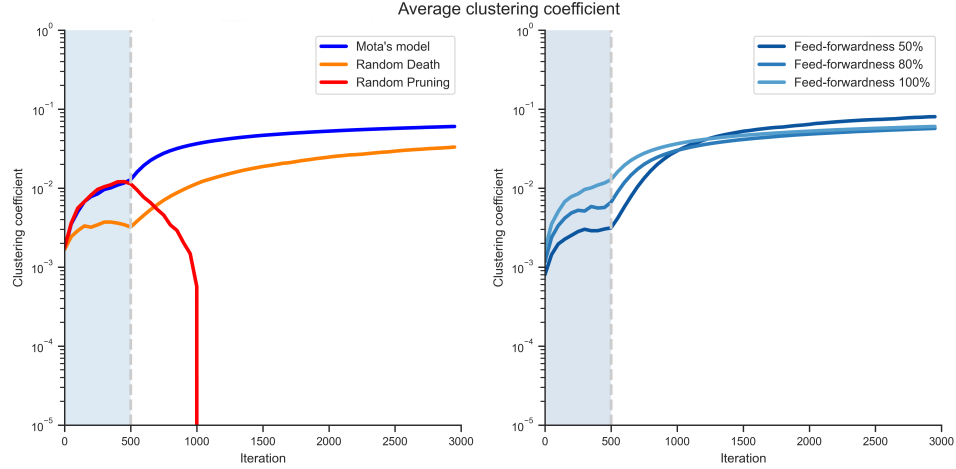


Figure 14: Evolution of the clustering coefficient in our model. (Left) Comparison with random death (orange) or random pruning (red). (Right) Various shades of blue indicate different degrees of feed-forwardness in the network, i.e. the percentage of regulatory connections. The shaded portion of the graph from 0 to 500 iterations represents the ND stage.

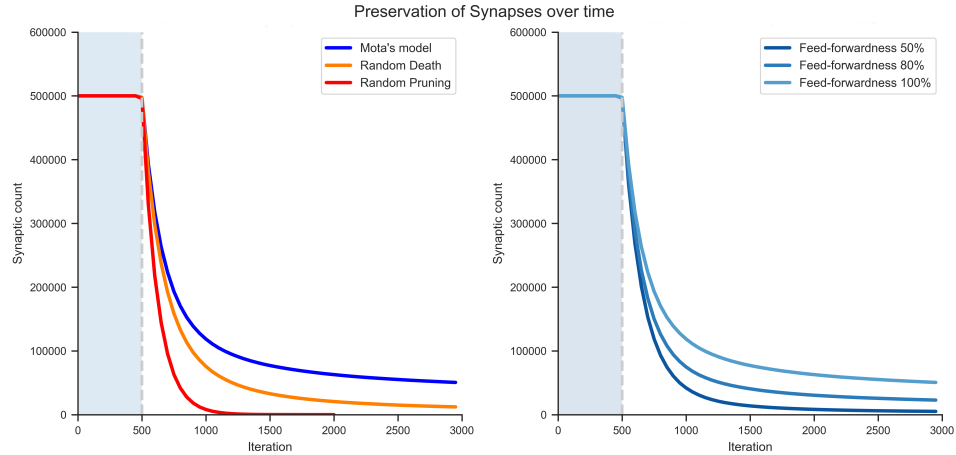


Figure 15: Number of synapses (edges) in the network as time progresses in the simulation. (Left) Comparison with random death (orange) or random pruning (red). (Right) Various shades of blue indicate different degrees of feed-forwardness in the network, i.e. the percentage of regulatory connections. The shaded portion of the graph from 0 to 500 iterations represents the ND stage.

Contrary to the main results with denser networks and longer iterations, in sparse networks selective pruning and neuronal death have a higher impact on preservation of network properties. The overall iteration time is shorter—3000 iterations—hence the network takes less time to stabilize leading to higher differences in network metrics between selective and random pruning conditions. Sparse networks are more prone to loss of their structural integrity than dense ones.

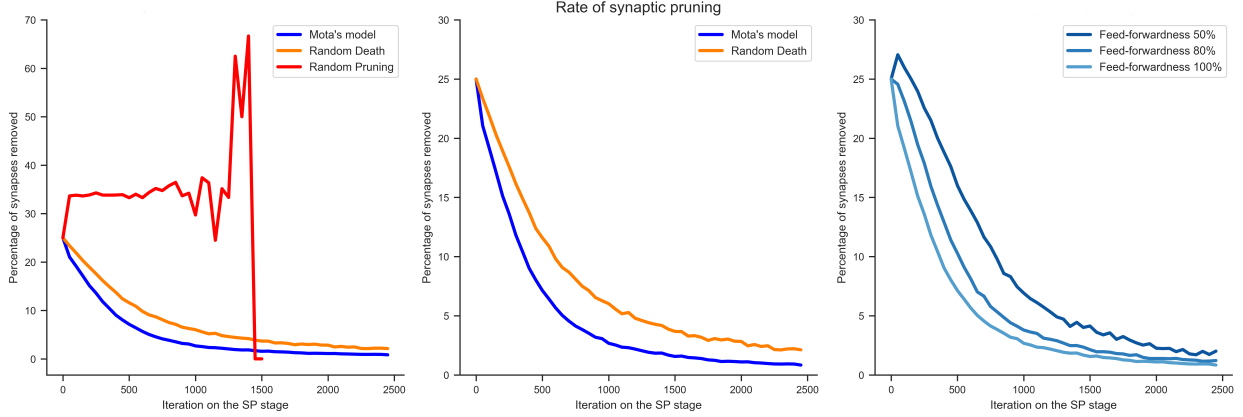


Figure 16: Percentage of connections (synapses) removed from the network per iteration of the simulation. (Left) Comparison with random death (orange) or random pruning (red). (Center) A closer look at the rates of synaptic pruning of the random death (orange) vs our model (blue). (Right) Various shades of blue indicate different degrees of feed-forwardness in the network, i.e. the percentage of regulatory connections.

Finally, Figure 17 shows that the degree of feed-forwardness affects the evolution of a network greatly. For instance, a high number of feed-forward connections leads to distribution that is much like that in the case of the base model, thus confirming an assertion made earlier about the significance of these feed-forward links in building scale-free networks. On the other hand, decreased levels of such connections have implications for the power law behaviour, suggesting a causal role for feed-forwardness in the generation of the final network (**50%**:  $D = 0.073$ ,  $\alpha = 1.827$ , at 2350 iterations; **80%**:  $D = 0.077$ ,  $\alpha = 1.692$ , at 2350 iterations; **100%**:  $D = 0.059$ ,  $\alpha = 1.693$ , at 2350 iterations).

Thus selective pruning and neuronal death play a vital role in constructing robust highly efficient scale-free neuron networks especially sparse ones with short evolution times; this relates to the findings above concerning development time as well as measures taken during the postnatal period. These observations not only provide insight into brain development but also disclose valuable ideas about network science suggesting that specific disconnecting mechanisms apply widely to building scale-free networks across different fields particularly when density is low and the time required for evolution is short-lived.

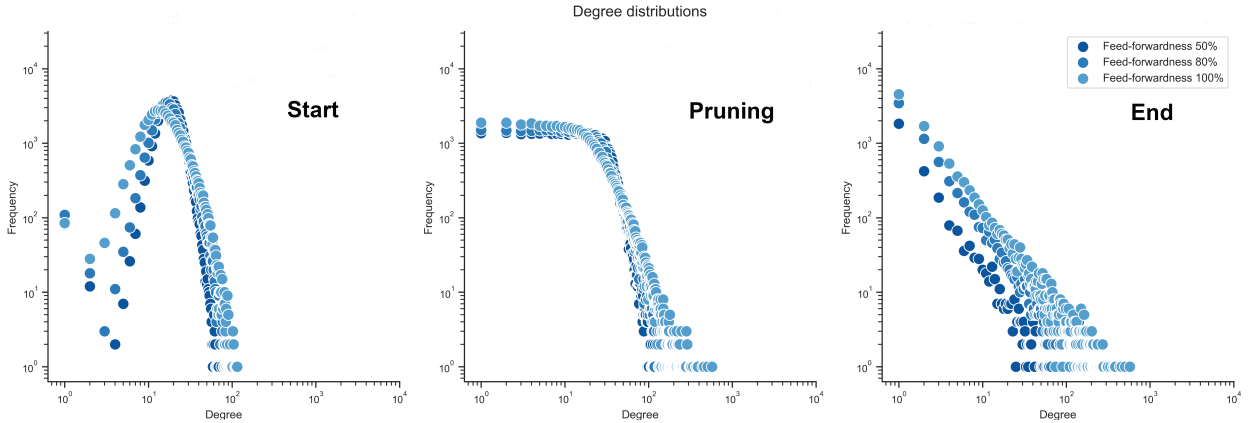


Figure 17: Distribution of the number of synapses (Degree) of each neuron (Node) in the network. The panels present the progression of the degree distribution in our model and shades of blue represent the different conditions tested, with blue representing different degrees of feed-forwardness in the network, i.e. the percentage of regulatory connections of 50% and 80%.